Conformational Analysis of Alkali Metal Salts of a Synthetic Carboxylic Ionophore by NMR Spectroscopy in Combination with X-ray Crystallography

Noriko C. Kasuga,[†] Hitoshi Kuboniwa,[‡] Seiichi Nakahama,[‡] and Kazuo Yamaguchi*,[†]

Contribution from the Department of Materials Science, Kanagawa University, Hiratsuka, Kanagawa 259-12, Japan, and Department of Polymer Chemistry, Faculty of Engineering, Tokyo Institute of Technology, Ohokayama, Meguro-ku, Tokyo 152, Japan

Received March 1, 1995[⊗]

Abstract: The solution structures of a linear synthetic carboxylic polyether ionophore, $HO[CH_2CH_2O(1,2\text{-}C_6H_4)O]_4\text{-}CH_2(1,2\text{-}C_6H_4)COOH$, **1**, and its alkali metal salts have been studied by ^1H and ^{13}C NMR spectroscopies ($^1H-^1H$ COSY, NOESY, $^{13}C-^1H$ COSY, HMQC, HMBC, and long range ^{13}C J resolved 2D-NMR). The ionophore **1** selectively transports K^+, Rb^+, and Cs^+ over Na^+ and Li^+. The ^1H NMR spectra of **1** and the Li and Na salts are simple, whereas those of K, Rb, and Cs salts are more highly chemical shift resolved but are very similar to each other. Conformational analyses of K, Rb, and Cs salts were carried out on the basis of the 3D structures in the crystal using vicinal three-bond coupling constants, NOE, and chemical shifts, which depend on the torsion angles of 1,2-ethylenedioxy, the distances between methylene and aromatic methyne protons, and the magnetic anisotropy mainly resulting from the aromatic rings, respectively. These data show good correlation with those expected from the structures in the crystal. The backbone bending observed in the crystals was also confirmed with chemical shifts and $^3J_{H-C}$ of ^{13}C NMR spectra of the K, Rb, and Cs salts. These results show that the conformation of K, Rb, and Cs salts which is similar to that in the crystal is dominant in a liquid membrane, but the Li and Na salts remain highly mobile in solution. These results are discussed in connection with the ion-transport ability of **1** through the liquid membrane.

Introduction

Supramolecular structures formed by noncovalent interactions such as hydrogen bonding, electrostatic interaction, and van der Waals forces have attracted increasing interest because their chemistry forms the basis for understanding biological processes at the molecular level such as substrate—receptor recognition, enzymatic reactions, and transport of substances, and for building molecular devices.[1] Host—guest complexes[1c] between organic host molecules and cation guests by dipole—ion interaction have been extensively studied as a representative example of the supermolecules since Pedersen discovered crown ethers.[2] Many cyclic host molecules, such as synthetic crown ethers and cryptands[3] as well as naturally occurring valinomycin and nonactin, have been reported.[4] This is because preorganization based on cyclic constraint is a great advantage in forming stable host—guest complexes.[1c,5] On the contrary, linear host compounds are not as frequently found as their cyclic counterparts.[6] Synthetic ionophores for ion-selective electrodes[7] and natural carboxylic ionophores[8] are examples of acyclic hosts. To build a wide variety of supramolecular structures, acyclic molecules are more attractive because their structures could be

modified more easily and would permit various supramolecular architectures with guests.[9] The elucidation of the spatial solution structures of such compounds and their host—guest complexes not only is essential to understand the complexation properties but also will provide insight for designing molecules. However, the flexible and relatively long main chains with many conformational possibilities make conformational analyses difficult.

As analogs of natural carboxylic ionophores such as monensin,[8b] we have synthesized a series of linear α-carboxy-ω-hydroxy polyethers.[10] Their backbones are composed only of repeating units derived from catechol and ethylene glycol instead of tetrahydrofuran and tetrahydropyran rings which are seen in

[†] Kanagawa University.

[‡] Tokyo Institute of Technology.

[⊗] Abstract published in *Advance ACS Abstracts,* June 15, 1995.

(1) (a) Lehn, J.-M. *Angew. Chem., Int. Ed. Engl.* **1988,** *27,* 90. (b) Lehn, J.-M. *Angew. Chem., Int. Ed. Engl.* **1990,** *29,* 1304. (c) Cram, D. J. *Angew. Chem., Int. Ed. Engl.* **1988,** *27,* 1009.
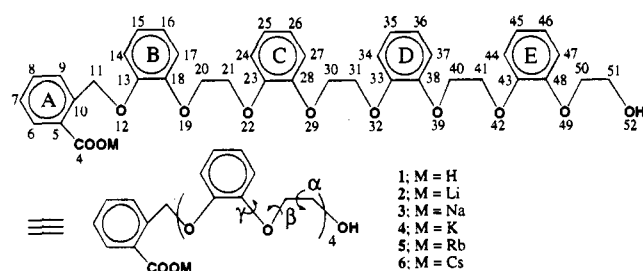
(2) (a) Pedersen, C. J. *J. Am. Chem. Soc.* **1967,** *89,* 2495. (b) Pedersen, C. J. *J. Am. Chem. Soc.* **1967,** *89,* 7017.

(3) Lehn, J.-M. *Structure and Bonding*; Springer-Verlag: Berlin, 1973; Vol. 16.

(4) (a) Ovchinnikov, Yu. A. *FEBS Lett.* **1974,** *44,* 1. (b) Pressman, B. C. *Annu. Rev. Biochem.* **1976,** *45,* 501.

(5) Cram, D. J.; deGrandpre, M. P.; Knobler, C. B.; Trueblood, K. N. *J. Am. Chem. Soc.* **1984,** *106,* 3286.

(6) (a) Takemoto, K.; Sonoda, N. In *Inclusion Compounds*; Atwood, J. L., Davies, J. E. D., Macnicol, D. D., Eds.; Academic Press: New York 1984; Vol. II, p 47. (b) E. Giglio, *Ibid.* p. 207. (c) Staudinger, H.; Döhle, W. *Makromol. Chem.* **1953,** *9,* 188.

(7) Ammann, D.; Morf, W. E.; Anker, P.; Meier, P. C.; Pretsch, E.; Simon, W. *Ion-Sel. Electrode Rev.* **1983,** *5,* 3.

(8) (a) Westley, W. J. In *Polyether Antibiotics Naturally Occurring Acid Ionophores*; Westley, J. W., Ed.; Marcel Dekker, Inc.: New York, 1982; Vol. 1, p 1 and references cited therein. (b) Lutz, W. K.; Winkler, F. K.; Dunitz, J. D. *Helv. Chim. Acta,* **1971,** *54,* 1103.

(9) (a) Vögtle, F.; Weber, E. *Angew. Chem., Int. Ed. Engl.* **1979,** *18,* 753. (b) Nabesima, T.; Inaba,T.; Furukawa, N. *Tetrahedron Lett.* **1987,** *28,* 6211. (c) Kobuke, Y.; Satoh. Y. *J. Am. Chem. Soc.* **1992,** *114,* 789. (d) Hiratani. K.; Sugihara, H.; Kasuga, K.; Fujiwara, K.; Hayashita, T.; Bartsch, R. A. *J. Chem. Soc., Chem. Commun.* **1994,** 319. (e) Iimori, T.; Still, W. C. *J. Am. Chem. Soc.* **1989,** 111, 3439.

(10) (a) Yamazaki, N.; Nakahama, S.; Hirao, A.; Negi, S. *Tetrahedron Lett.* **1978,** *27,* 2429. (b) Yamazaki, N.; Hirao, A.; Nakahama, S. *J. Macromol. Sci. Chem.* **1979,** *A13,* 321. (c) Kuboniwa, H.; Yamaguchi, K.; Hirao, A.; Nakahama, S.; Yamazaki, N. *Chem. Lett.* **1982,** 1937. (d) Kuboniwa, H.; Nagami, S.; Yamaguchi, K.; Hirao, A.; Nakahama, S.;Yamazaki, N. *J. Chem. Soc., Chem. Commun.* **1985,** 1468. (e) Yamaguchi, K.; Negi, S.; Kuboniwa, S.; Kozakai, S.; Nagano, R.; Kuboniwa, H.; Hirao, A.; Nakahama, S.; Yamazaki, N. *Bull. Chem. Soc. Jpn.* **1988,** *61,* 2047. (f) Yamaguchi, K.; Kuboniwa, H.; Murakami, N.; Hirao, A.; Nakahama, S.; Yamazaki, N. *Bull. Chem. Soc. Jpn.* **1989,** *62,* 1097.
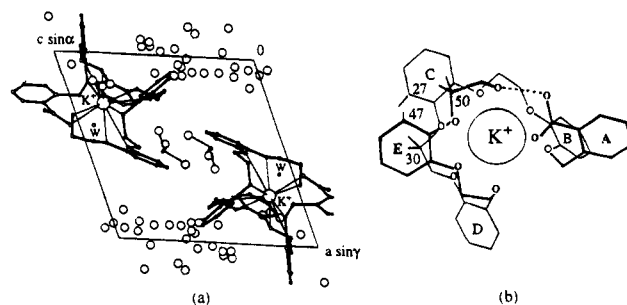
Chart 1

Figure 1. Crystal structure of $4 \cdot 2H_2O \cdot CHCl_3$ viewed down the b axis determined by X-ray diffraction (a) and the molecular structure (b) of **4**.[15] The large circles indicate the Cl atom of the disordered $CHCl_3$ molecules.

natural ionophores.[8] Among the synthetic ionophores, 2-[[2-[2-[2-[2-[2-[2-(2-hydroxyethoxy)phenoxy]ethoxy]phenoxy]-ethoxy]phenoxy]ethoxy] phenoxy]methyl]benzoic acid, **1**, consisting of 30 atoms in the backbone, exhibits high transport K^+, Rb^+, and Cs^+ over Na^+ and Li^+ through a 1, 2-dichloroethane liquid membrane.[10d,11] In this paper we describe the studies of solution conformations of **1** and its Li, Na, K, Rb, and Cs salts (**2—6**, respectively) (Chart 1) based on NMR data on the basis of the crystal structures and discuss them in connection with the ion-transporting properties of **1**.

Conformational studies have been performed mainly by NMR spectroscopy analyzing the torsion-angle-dependent three-bond coupling constants and distance-dependent nuclear Overhauser effect, NOE.[12] These parameters have provided whole solution structures of large molecules such as proteins, taking into account van der Waals repulsion after sequential assignments using 2D-NMR were performed.[13] However, the solution structures of oligomeric open-chain compounds such as peptides,[14] our synthetic ionophores, and their salts cannot be determined only by the techniques developed for large molecules because the number of ^3J and NOEs is too few compared to the number of possible conformations.

We determined the crystal structures of **4—6**.[15] The molecular structures of **4—6** are very similar to each other. Figure 1 shows the crystal and molecular structures of **4** as an example. The backbone of **4—6** forms pseudocycles by head-to-tail hydrogen bonding between the terminal carboxyl and hydroxyl groups and basically adopts a conformation like the seam of a tennis ball, resulting in the formation of cavities fitted for the size of each cation. In the crystal, salt molecules of **4—6** are separated by chloroform molecules used for crystallization, resulting in weak intermolecular interactions. The solvent molecules are highly disordered, having large temperature factors. In addition, another crystal form is obtained for **5**, revealing the same molecular structure.[16] It is worth comparing the observed NMR data as much as possible with those expected by the structures in the crystal because the backbone of these salts would have some flexibility in solution.

The conformation of the salts is described by three torsion angles, α, β, and γ, which are illustrated in Chart 1. The α

angles can be obtained from $^3J_{H-H}$. The β angles should be estimated from either $^3J_{C-H}$ of $H-C(sp^3)-O-C$(quaternary carbon, sp^2) linkage or $^3J_{C-C}$ of $C(sp^3)-C(sp^3)-O-C$(quaternary carbon, sp^2). The former can be observed, but the value is often small.[17] The latter is very hard to obtain because of the poor ^{13}C atom abundance. Although the γ angles could not be determined from $^3J_{C-C}$, they are analyzed from the NOE between protons in $H-C(sp^2)-C$(quaternary carbon, sp^2)$-O-C(sp^3)-H$. The number of observed NOE interactions through space is too few to build the 3D structures of the three salts. Chemical shifts reflect the 3D structures in solution because they are sensitive to the magnetic anisotropy of the aromatic rings, carbonyl group, and charges. They are generally used to account for local environments of molecules such as cyclophanes[18] and proteins.[19] However, studies of solution conformation based on the chemical shifts are relatively rare compared to those from ^3J and NOE data. Because of the alternating aromatic rings in the backbone, the chemical shifts of **1** and its salts should serve as a probe of the solution structures. In the crystal, H27, H30, H47, and H50 are located in the shielding region of the E, E, C, and C aromatic rings, respectively. If the solution structures of **4—6** resemble those in the crystal, the signals of these protons should be shielded and appear upfield.[20] The local anisotropic contribution to the chemical shifts for the 1,2-ethylenedioxy and 1,2-phenylene-dioxy protons by the aromatic rings, the carboxyl group, and the alkali metal ion is estimated on the basis of the structures in the crystal. The calculated chemical shifts are compared with the observed ones. The chemical shifts of carbon are sensitive to conformational change and the steric effects of the backbone.[17] If the backbone of **4—6** is bending in solution as observed in the crystal, the chemical shifts near the kink will be shifted. The $^3J_{H-C}$ for that part will also be measurable.[17,21]

We made a preliminary report of the ^1H NMR spectra and conformational analyses of **1**, **3**, and **4** without any X-ray data.[10d,22] Herein, studies on the solution conformations of **1—6** with NMR data which are analyzed in more detail by the strategy mentioned above are presented and they are discussed

(11) Yamaguchi, K.; Kuboniwa, H.; Nagami, S.; Bando, T.; Hirao, A.; Nakahama, S.; Yamazaki, N. *Bull. Chem. Soc. Jpn.* **1995**, *68*, 315.

(12) (a) Anteunis, M. J. O. In *Polyether Antibiotics Naturally Occurring Acid Ionophores*; Westley, J. W., Ed.; Marcel Dekker, Inc.: New York, 1982; Vol. 2. p 245. (b) Beloeil, Jean-Claude; Bious, V.; Dauphin, G.; Garnier, J.; Morellet, N.; Vaufrey, F. *Magn. Reson. Chem.* **1994**, *32*, 83. (c) Seto, H.; Otake, N. In *Polyether Antibiotics Naturally Occurring Acid Ionophores*; Westley, J. W., Ed.; Marcel Dekker, Inc.: New York, 1982; Vol. 2, p 335.

(13) Wüthrich, K. *NMR of Proteins and Nucleic Acids*; John Wiley & Sons: New York, 1986.

(14) Williamson, M. P.; Waltho, J. P. *Chem. Soc. Rev.* **1992**, 227.

(15) (a) Kuboniwa, H.; Yamaguchi, K.; Nakahama, S.; Hori, K.; Ohashi, Y. *Chem. Lett.* **1988**, 923. (b) Kasuga, N.; Nakahama, S.; Yamaguchi, K.; Ohashi, Y.; Hori, K. *Bull. Chem. Soc. Jpn.* **1991**, *64*, 3548.

(16) The unit cell dimensions of *a*, *b*, *c*, α, β, γ, and *V* are 13.482 Å, 13.581 Å, 16.434 Å, 82.345°, 109.55°, 112.75°, and 2615.1 Å^3, respectively.

(17) Marshall, J. L. *Carbon-Carbon and Carbon-Proton NMR Couplings, Methods in Stereochemical Analysis*; Verlag Chemie: Weinheim, Germany, 1983; Vol. 2, p 20.

(18) (a) Mitchell, R. H. In *Cyclophanes I*; Keehn, P. M., Rosenfeld, S. M., Eds.; Academic Press: New York, 1983; p 239. (b) Fukazawa, Y.; Usui, S.; Tanimoto, K.; Hirai, Y. *J. Am. Chem. Soc.* **1994**, *116*, 8169.

(19) (a) Wüthrich, K.; Wider, G.; Wagner, G.; Braun, W. *J. Mol. Biol.* **1982**, *155*, 311. (b) Williamson, M. P. *Biopolymers* **1990**, *29*, 1423.

(20) However, the coiled conformation we proposed previously[22] does not predict such chemical shift behavior.

(21) Breitmaier, E.; Voelter, W. *^{13}C NMR Spectroscopy, Methods and Applications in Organic Chemitry*, 2nd ed.; Verlag Chemie: New York, 1978; p 92.

(22) Kuboniwa, H.; Yamaguchi, K.; Hirao, A.; Nakahama, S.; Yamazaki, N. *Magn. Reson. Chem.* **1986**, *24*, 961.
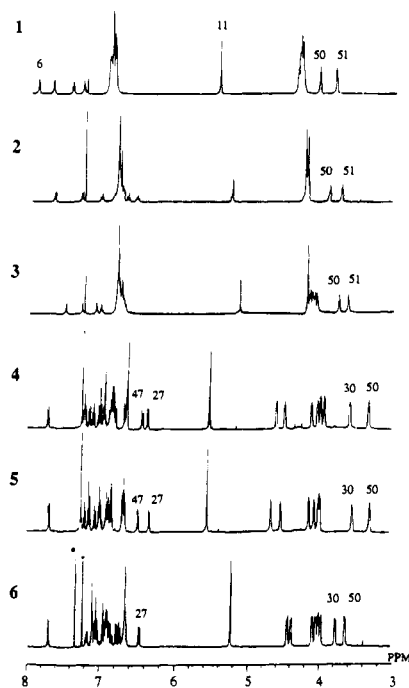
Figure 2. ^{1}H NMR spectra of **1–6** measured in CDCl$_3$. The asterisk shows the signal of benzene used for freeze-drying.

in connection with the ion-transporting abilities of **1**. We briefly discuss solid-state ^{13}C NMR spectra of **1** and **4**.

Results and Discussion

^{1}H NMR Spectra. Figure 2 shows the ^{1}H NMR spectra of **1–6** in CDCl$_3$. The relatively simple spectra of **1–3** mean that rapid interconversion between a large number of conformers takes place on the NMR time scale in solution.

The spectra of **4–6**, which are significantly different from those of **1**, show the multiplicity and separation in the 1,2-ethylenedioxy moiety and the 1,2-phenylenedioxy ring. This multiplicity and separation are due to certain solution structures. The contribution of magnetic anisotropy on chemical shifts caused by the aromatic rings, the carbonyl group, and the electric field of M$^+$ and COO$^-$ differs for the 3D structure. Signals of H27, H30, H47, and H50 in the ^{1}H NMR spectra of **4–6** shift to the upper field compared to those of **1**. These shifts of protons seem to be explained by shielding of the E, E, C, and C aromatic rings, respectively, in the crystal as depicted in Figure 1. This will be discussed below.

The partial assignments of **1–3** were done according to the chemical shifts of analogs. The chemical shifts of **4–6** were determined by sequential resonance assignments from ^{1}H–^{1}H COSY and NOESY spectra. The assignments were carried out from the terminal 2-hydroxyethoxy protons (H51) which have no correlation peak with the aromatic protons in the NOESY spectra. The signals of the aromatic protons in the 4- and 5-positions which have correlation peaks with both resonances in the 3- and 6-positions in ^{1}H–^{1}H COSY spectra were assigned by ^{13}C–^{1}H COSY/^{1}H-detected multiple quantum coherence (HMQC) and heteronuclear multiple bond correlation (HMBC) spectra.[23] However, some of them could not be determined because of the resonance-overlapping. Another sequential assignment starting from H6 which is located near the other terminal carboxyl group also gives the same results.

The spectrum of **3** is strongly influenced by the water content of the solvent. When a drop of D$_2$O is added to the solution,

(23) Summers, M. F.; Marzilli, L. G.; Bax, A. *J. Am. Chem. Soc.* **1986**, *108*, 4285.
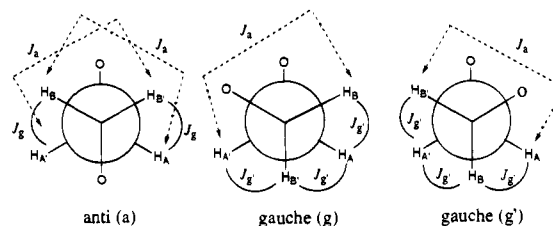

Figure 3. Newman projections of the three conformers obtained by internal rotation about the carbon—carbon bond of the 1,2-ethylenedioxy group.

the spectrum becomes similar to that of **2**. The water content of CDCl$_3$ hardly influences the spectrum of **4**. These spectral changes correspond with data for the interfacial tension and dynamic light scattering for **3** and **4**.[11]

(a) Vicinal Coupling Constants of 1,2-Ethylenedioxy Relating to the α Angle. The methylene signals are split according to the vicinal coupling of the four-spin AA'BB' system except for those of the inner methylene protons of **1–3** which are gathered to form one broad signal in each spectrum. The vicinal coupling constants, J_{AB} and $J_{AB'}$, are obtained by simulating the spectra of 1,2-ethylenedioxy protons using a LAOCOON-type program.[24] Under the assumption that the conformation around the H$_A$H$_A'$C—CH$_B$H$_B'$ bond in solution comprises three types of the preferred conformers denoted by anti (a) and gauche (g and g') as shown in Figure 3, the fractional populations, f_a, f_g, and $f_{g'}$, are calculated.

Assuming the rapid internal conversion among these conformers in solution, the observed J_{AB} and $J_{A'B}$ values are time-averaged over the three preferred conformers as expressed in terms of f_a, f_g, $f_{g'}$, J_a, J_g, and $J_{g'}$ in eqs 1 and 2, where J_a and $J_{g'}$

$$J_{AB} = f_a J_a + (f_g + f_{g'})J_{g'} \tag{1}$$

$$J_{A'B} = f_a J_g + f_g J_a + f_{g'} J_{g'} \tag{2}$$

$$f_a + f_g + f_{g'} = 1 \tag{3}$$

for the coupling constants in anti and gauche arrangement are 14.0 and 2.1 Hz, respectively, for H20 to H41 derived from a modified Karplus type equation.[25] In a similar manner, J_a and $J_{g'}$ for H50 and H51 are 14.0 and 2.2 Hz, respectively. Conformational distributions of the three conformers are estimated with the observed vicinal coupling constants, J_{AB} and $J_{A'B}$, from eqs 4 and 5 derived from eqs 1 and 3.

$$f_a = \frac{(J_{AB} - J_{g'})}{(J_a - J_{g'})} \tag{4}$$

$$f_g + f_{g'} = 1 - f_a \tag{5}$$

For **1–3**, distributions were calculated only for the well-separated terminal 2-hydroxyethoxy unit. The observed coupling constants and rotamer populations are listed in Table 1. Because we could not tell which carbon is facing the head or tail in each 1,2-ethylenedioxy unit as shown in Figure 3, the f_a and the total values of the gauche fraction (f_g and $f_{g'}$) are presented.

The predominance of gauche conformers (> 90%) over anti ones is seen for all data of **1–6** as seen in poly- or oligo(ethylene

(24) (a) Castellano, S.; Bothner-By, A. A. *J. Chem. Phy.* **1964**, *41*, 3863. (b) Detar, D. F. *Computer Programs for Chemistry*. W. A. Benjamin, Inc.: New York, 1968; Vol. 1, p 10.

(25) Colucci, W. J.; Jungk, S. J; Gandour, R. D. *Magn. Reson. Chem.* **1985**, *23*, 335.

Table 1. Vicinal Coupling Constants and Rotamer Populations of **1−6** in CDCl₃

compd	proton no.	$J_{AA'}, J_{BB'}$ (Hz)	$J_{AB}, J_{A'B'}$ (Hz)	$J_{AB'}, J_{A'B}$ (Hz)	$f_g + f_{g'}$ (%)	f_a (%)
1	50−51	−10, −10	3.3	5.4	90	10
2	50−51	−10, −10	3.3	5.4	90	10
3	50−51	−10, −10	3.3	5.5	90	10
4	20−21	−10, −10	2.5	6.3	97	3
	30−31	−10, −10	2.2	6.3	99	1
	40−41	−10, −10	2.3	5.5	98	2
	50−51	−10, −10	2.9	5.3	94	6
5	20−21	−10, −10	2.3	6.2	98	2
	30−31	−10, −10	2.1	6.2	100	0
	40−41	−10, −11	2.3	5.4	98	2
	50−51	−10, −10	3.0	5.3	93	7
6	20−21	−10, −10	2.4	6.4	97	3
	30−31	−10, −10	2.2	6.4	99	1
	40−41	−10, −10	2.2	6.7	99	1
	50−51	−10, −10	3.0	5.3	93	7

Table 2. Intensity Enhancement and Distances of Protons, r,[a] in the Crystal

irradiated proton	NOE	4 NOE obsd (%)	4 r (Å)	5 NOE (%)	5 r (Å)	6 NOE (%)	6 r (Å)
H11	H9	15	2.19, 3.21	5	2.48, 3.51	14	2.28, 3.49
H11	H14	20	2.01, 3.42	9	2.04, 3.47	19	1.88, 3.53
H20	H17	32	2.14, 2.38	17	2.27, 2.36	26	2.23, 2.29
H21	H24	27	2.17, 2.15	22	2.18, 2.53	22	1.94, 2.21
H30	H27	26	2.18, 2.71	21	2.37, 2.43	25	2.07, 2.29
H31	H34	46	2.10, 2.47	22	2.18, 2.30	21	1.90, 2.24
H40	H37	17	2.58, 3.60	13	2.35, 3.53	20	2.27, 3.86
H41	H44	26	2.40, 2.65	19	2.13, 2.51	23	1.60, 2.63
H50	H47	27	2.34, 2.37	20	2.24, 2.31	24	2.18, 2.36
H20	H21	11	1.97−2.61	5	2.29−2.99	4	2.32−3.00
H21	H20	6	1.97−2.61	9	2.29−2.99	7	2.32−3.00
H30	H31	5	2.33−2.97	4	2.29−3.00	6	2.47−3.05
H31	H30	8	2.33−2.97	6	2.29−3.00	4	2.47−3.05
H40	H41	7	2.30−2.96	6	2.35−3.01	7	1.79−2.98
H40	H11	2	2.71−4.18	1	3.04−4.74	0	4.13−5.74
H41	H40	12	2.30−2.96	6	2.35−3.01	6	1.79−2.98
H50	H51	9	2.34−3.10	7	2.21−2.99	4	2.16−2.91
H51	H50	7	2.34−3.10	7	2.21−2.99	5	2.16−2.91

[a] For methylene protons, r_{max} and r_{min} are displayed among the four r's.

oxides),[26ab] crown ethers,[26c] and their complexes.[26d] For **4−6**, the gauche richness is also in accord with the molecular structures in the crystal. The gauche fraction of C50−C51 which is located close to the terminal hydroxyl group is slightly smaller in all cases than those of the other three 1,2-ethylenedioxy pairs, C20−C21, C30−C31, and C40−C41, which could indicate that the terminal ends have a little more rotational freedom.

(b) Differential NOE Experiment Relating to the β and γ Angles. Differential NOE experiments of **4−6** were carried out to estimate the ¹H−¹H internuclear distance (r) pertaining to the β and γ angles. Only aliphatic protons were irradiated to measure the NOE because they were sufficiently separated from each other, except for H20 and H41 of **6**. Table 2 lists the intensity enhancement as well as the maximum and minimum values of one or two pairs of r evaluated from the structures in the crystal. It is difficult to obtain an adequate number of NOEs for **4−6** to build the 3D structures because the backbone is composed of the repeating polyether units. Distances between the protons for which NOEs are observed

(a)　　　　　　　　　　　　(b)
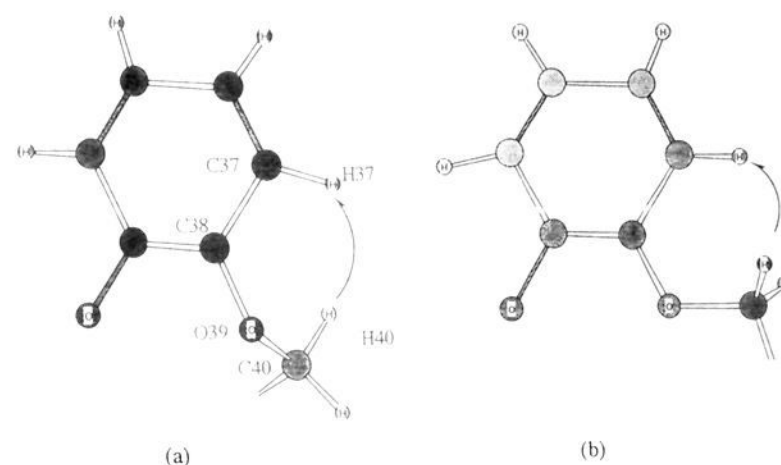
Figure 4. Conformation around the C37−C38−O39−C40 angle (a) and the other C−C−O−C angles (b).

are within 3 Å in the structures determined in the crystal.[15] The observed NOE between H11 and H40, regardless of the weak intensity, indicates that these protons are close to each other through space, which is consistent with conformations in the solid. The enhancement for aliphatic protons is not as large as that for aromatic ones because efficient cross-relaxation between the closely spaced geminal methylene protons must take place for the methylene protons.[27] Intensities of NOE observed between aromatic protons and methylene protons become smaller for those of H9 {H11}, H14 {H11}, and H37 {H40} than those of the others which have one large r value (>3 Å) in the pair. These data are in agreement with backbone-bending structures in the crystal (Figure 4). The observed NOE of **4−6** shows good correlation with the molecular structures in the solid.

(c) Comparison of Observed and Calculated ¹H NMR Chemical Shifts, Relating to the α, β, and γ Angles. The chemical shifts are often used to predict the local conformation for compounds containing aromatic rings in particular.[18,19] However, they are not widely used to obtain the whole molecular structures of macrocycles and open-chain compounds.

The separation of resonances in the spectra of **4−6** should result from the magnetic anisotropy of the aromatic rings, carbonyl group, and electric field arising from M⁺ and COO⁻ of the time-averaged structures. Their chemical shifts seem to be in agreement with those expected from the crystal structures depicted in Figure 1. Thus, these effects of **4−6** are quantitatively evaluated on the basis of the structures in the crystals. The induced chemical shifts of **4−6** ($\Delta\delta$) were calculated as the summation of the magnetic anisotropy of the five aromatic rings ($\Delta\delta_R$), carbonyl group ($\Delta\delta_{C=O}$), and electric field provided by M⁺ and COO⁻ ($\Delta\delta_E$) using the methods of Johnson−Bovey,[28a] ApSimon,[28b] and Chan,[26c] respectively. In the calculation of $\Delta\delta_{C=O}$, the values of magnetic susceptibilities were taken from the report of Zücher.[28c] To calculate the chemical shifts (δ_{calcd}), the standard chemical shifts are added to $\Delta\delta$ which are chosen as follows: The values of 3.60 ppm for the inner 1,2-ethylenedioxy protons (H20 to H41) and 3.53 ppm for the outer methylene protons (H50) are selected as the standard taken from ethylene glycol diethyl ether and 2-ethoxyethanol, separately.[29] Because two methylene protons appear as one broad AA'BB' signal, the two chemical shifts calculated are averaged. For the aromatic protons in the 1,2-phenylenedioxy ring, 6.89 ppm was chosen as a standard value from the ion-free spectrum

(26) (a) Mark, J. E.; Flory, J. *J. Am. Chem. Soc.* **1966**, *88*, 3702. (b) Tadokoro, H; Chatani, Y.; Yoshihara, T.; Tahara, S.; Murahashi, S. *Makromol. Chem.* **1964**, *73*, 109. (c) Live, D.; Chan, S. I. *J. Am. Chem. Soc.* **1976**, *98*, 3769. (d)Iwamoto, R.; Wakano, H. *J. Am. Chem. Soc.* **1976**, *98*, 3764.

(27) Neuhaus, D.; Williamson, M. P. *The Nuclear Overhauser Effect in Structural and Conformational Analysis*; VCH Publishers, Inc.: New York, 1989; p 63.

(28) (a) Johnson, C. E., Jr.; Bovey, F. A. *J. Chem. Phys.* **1958**, *29*, 1012. (b) ApSimon, J. W.; Craig, W. G.; Demarco, P. V.; Mathieson, D. W.; Saunders, L. *Tetrahedron* **1967**, *23*, 2357. (c) Zürcher, R. F. *Prog. NMR Spectrosc.*, 1967, *2*, 205.

(29) Sakai, S. *Handbook of Proton-NMR Spectra and Data*; Academic Press: New York, 1985; Vol. 1−5.

Table 3. Observed and Calculated Chemical Shifts of **4−6** (ppm)

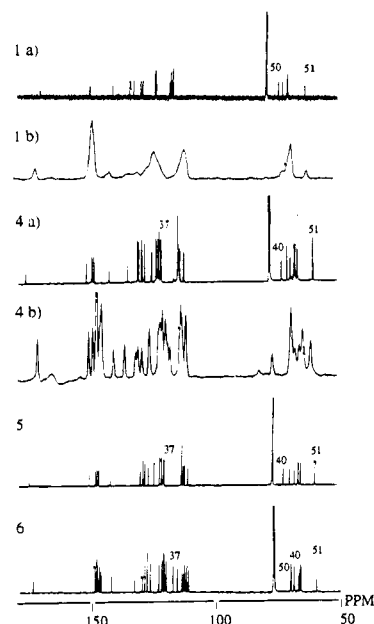|	4		5		6	
proton	δ_{calcd}	$\delta_{obsd} - \delta_{calcd}$	δ_{calcd}	$\delta_{obsd} - \delta_{calcd}$	δ_{calcd}	$\delta_{obsd} - \delta_{calcd}$
H14	7.04	−0.19	7.13	−0.24	7.17	−0.23
H15	6.77	0.08	6.83	−0.01−0.03[a]	6.84	−0.15 to ∼−0.14[a]
H16	6.71	−0.06	6.80	0.02−0.06[a]	6.80	−0.11 to ∼−0.10[a]
H17	6.69	−0.04	6.79	−0.12	6.77	−0.07
H24	7.13	−0.16	7.15	−0.15	7.14	−0.16
H25	7.12	−0.16	7.14	−0.18	7.13	−0.18
H26	7.11	−0.25	7.15	−0.27	7.14	−0.26
H27	6.61	−0.26	6.57	−0.24	6.19	0.31
H34	6.82	−0.02	6.86	−0.03	7.03	−0.23
H35	6.86	−0.19	6.91	0.14	6.76	0.32
H36	7.02	−0.03	6.99	0.00	6.87	0.19
H37	7.31	−0.21	7.22	−0.10	7.19	−0.14
H44	6.98	−0.31	6.94	−0.26	6.87	−0.12
H45	7.00	−0.17	7.01	−0.19	7.02	−0.16
H46	7.05	−0.20	7.09	−0.23	7.09	−0.19
H47	6.74	−0.29	6.62	−0.14	6.63	−0.06
H20	4.25	−0.14	4.26	−0.13	4.24	−0.18
H21	4.45	0.03	4.35	0.17	4.40	−0.02
H30	3.02	0.56	2.99	0.54	3.06	0.75
H31	4.08	−0.05	4.04	0.02	4.15	−0.15
H40	4.48	0.11	4.44	0.21	4.35	0.08
H41	4.04	−0.05	3.97	0.01	4.05	0.05
H50	2.72	0.61	2.55	0.74	2.65	1.02

[a] The protons in the 4- and 5-positions are not distinguishable in 2D-NMR measurements.
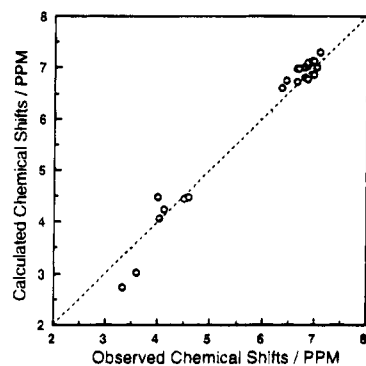
Figure 5. Relationship of the observed and calculated chemical shifts of the aromatic and 1,2-ethylenedioxy protons of **4**.

Figure 6. ¹³C NMR spectra of **1** and **4** in CDCl₃ (a) and in the solid (b) with those of **5** and **6** in CDCl₃ solution.

of **1** containing the ring current effect of the attached 1,2-phenylenedioxy ring. The standard value for the 1,2-phenylenedioxy protons was considered to contain ring current effects only from the attached 1,2-phenylenedioxy ring because the effects from the other 1,2-phenylenedioxy rings would be totally zero. Hence, the magnetic anisotropies of the other aromatic rings and the carbonyl group as well as the effects from M^+ and COO^- are added to 6.89 ppm to give the calculated values. The observed chemical shifts, except for that of terminal H51 which is considerably influenced by intramolecular hydrogen bonding, are compared with the calculated ones as shown in Table 3. The signals are well assigned with 2D-NMR, and the chemical environment is equivalent aside from the conformational effects. The observed and calculated chemical shifts of **4** are illustrated in Figure 5 as an example.

The calculation shows that large upper-field shifts of H27, H30, H47, and H50 arise from ring-current effects of the E, E, C, and C aromatic rings, respectively (data not shown). The magnetic anisotropy of the carbonyl group seldom affects the chemical shifts except for the terminal H6 and H51. It is clear that the ring-current mainly influences the chemical shifts of the selected protons. The calculated chemical shifts of aliphatic and aromatic protons for **4** agree with the observed values.

The difference between the observed chemical shifts (δ_{obsd}) and the calculated ones (δ_{calcd}) for **4−6** is within 0.4 ppm for

aromatic protons and 1.1 ppm for methylene ones as shown in Table 3. The difference is relatively large for the aliphatic protons of **4−6**, H30 and H50, as well as the aromatic proton of **6**, H27 in the table. For methylene protons, this difference would be due to contribution of the other gauche conformers, g or g′. The degree of such an effect would be larger for H30 and H50 which are more strongly influenced by ring-current effects than the others. The aromatic H27 of **6** in the crystal should be considerably shielded by the ring current because the proton is closer to the E ring horizontally. On the whole, our simple models evaluating the effects of magnetic anisotropy and electric fields explain the observed chemical shifts. This indicates that the relative spatial arrangements of the dominants of **4−6** are similar to those in the crystal although the molecules are fluctuating in solution. The complexes of alkali metal ions with crown ethers also have solution structures similar to those in the crystal, but some of 3D structures of crown ether without salts are different from those in the crystalline state.[26c,30] It seems that the molecular structure of **6** in the crystal is less retained in solution than that of **4** and **5**. However, we have no more evidence for more precise spectral interpretation.

¹³C NMR Spectra. (a) Spectra in Solution. The backbone bending of **4−6** was investigated by their chemical shifts from $^1H-^{13}C$ COSY and HMQC spectra and by $^3J_{C-H}$ from long range ¹³C J resolved 2D-NMR (LRJR)[31] and HMBC spectra. Complete decoupled ¹³C NMR spectra of **1, 4, 5,** and **6** in CDCl₃ are shown in Figure 6.

In the ¹³C NMR spectrum of **1**, the signals were overlapping as was seen in the ¹H NMR spectrum. By taking selectively proton-decoupled ¹³C NMR spectra, C11, C50, and C51 were identified and the signals of C4, C5, and C10 were assigned according to the chemical shifts of the analogs. The other peaks could not be assigned, because satisfactory assignment of the ¹H NMR spectra was difficult as described above. Most of the carbon signals of **4−6** appear separately, and the spectra are similar to each other. The carbons of **4−6** bonded to protons were identified using the ¹³C−¹H COSY and HMQC spectra with the knowledge of the chemical shifts of the protons described above. The quaternary carbons, C4, C5, and C10,

(30) Shamsipur, M.; Popov, A. I. *J. Am. Chem. Soc.* **1979**, *101*, 4051.
(31) Bax, A.; Freeman, R. *J. Am. Chem. Soc.* **1982**, *104*, 1099.

Alkali Metal Salts of a Synthetic Carboxylic Ionophore

J. Am. Chem. Soc., Vol. 117, No. 27, 1995 7243

were identified on the basis of chemical shifts of the analogous compounds and also from HMBC spectra. Except for C40 and C50, the aliphatic carbons of **4−6** are upfield shifted in comparison to those of **1**. Upfield shift upon coordination with alkali metal ions is also seen in crown ethers.[26c,30] The lower-field shifts of C40 may be qualitatively explained by the angular dependence of ^{13}C shielding for the methyl group of anisole.[32] The calculation (ab initio) using a localized orbital local origin indicates that the sp^3 carbon is strongly deshielded around 90°. For **4−6**, the torsion angle of C37−C38−O39−C40 is about −75°. The resonance of C40 shifts to the lower field on coordinating with K^+, Rb^+, and Cs^+. The degree of the downfield shift is larger for the K and Rb salts than that for the Cs salt. However, C40 appears at the same place with the other signals of the inner secondary carbons for the free acid and Na salt. The signal of C37 for the three salts shifts about 5 ppm lower from that of **1** and appears in the region of carbon at the 4- and 5-positions. The chemical shift of C37 shows a value similar to that for strained cyclic 1,2-dialkoxybenzenes whose aryl−O−C torsion angle is also bending, whereas the others at the 3- and 6-positions have values close to that of mobile 1,2-dimethoxybenzene.[33] These downfield shifts could be due to the backbone bending. So far, we cannot explain the lower shift of C50, although intramolecular hydrogen bonding may have some influence on it.

The relationship between the three-bond C−H coupling constants ^3J ($^{13}C−O−C−H$) and the dihedral angle of ^{13}C and ^1H is given by a Karplus-type equation rather qualitatively compared with that of $^3J(H−C−C−H)$.[17] The values of $^3J(^{13}C−O−C−H)$ provide information about the dihedral angles of the C−O bond and show a maximum if the dihedral angle between ^{13}C and H is 0° and 180°, while an angle of 90° presents a minimum ^3J value based on the Karplus relationship. After we made sure that the experiments give $^3J_{C−H}$, not $^2J_{C−H}$, using 1,2-diethoxybenzene, LRJR spectra were measured by irradiating the methylene protons, H11, H20, H21, H30, H31, H40, H41, H50, and H51. The LRJR experiments of **4** show only one triplet at C38 by irradiation of H40 as shown in Figure 7. In the HMBC spectra of **4**, the correlation peak was also observed only between H40 and C38.

In the crystal of **4**, the molecular bending at O39 makes the two dihedral angles of the H−C−O−C linkage 22° and 142°, whereas the other conformation of H−C−O−C is gauche whose $^3J_{H−C}$ may be too small to be observed. These results of the LRJR and HMBC spectra of **4** agree with the structures in the crystal. $^3J_{H11−C13}$ is also considered to be large enough to be observed, but we could not observe it. This may be due to the different structure of the terminal benzoate unit. For **5** and **6**, the same results are obtained from HMBC spectra. The chemical shifts and $^3J_{H−C}$ indicate that the backbone of **4−6** is bending in solution.

(b) Spectra in Solid. The ^{13}C NMR spectra of **1** and **4** in the solid are depicted in Figure 6. The spectrum for **1** shows a broad, simple pattern whereas that for **4** displays a sharp, complicated pattern. This drastic change in spectra should not be explained only by the electrical effects of potassium ion. These spectra indicate that the conformational change occurs when **1** coordinates with K^+. That is consistent with the spectral changes which are seen in the ^1H and ^{13}C NMR spectra in solution. Assignment of the signals of **1** and **4** was done on the basis of solution NMR spectra. Because the ionophore consists only of similar types of carbons resulting from repeating
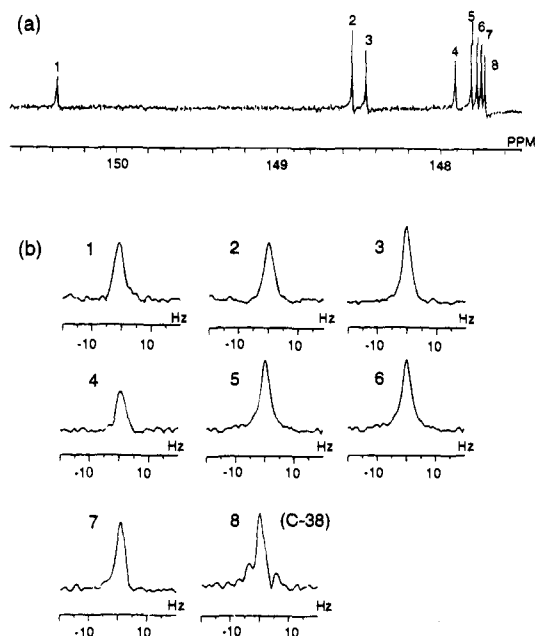

Figure 7. Proton noise decoupling ^{13}C NMR spectra of **4** (a) and LRJR spectra of **4** with irradiation of H40 (b) in $CDCl_3$ at 40 °C.

ether units and line-broadening occurs, it is difficult to fully assign each resonance in the solid NMR spectra.

We refer to reported NMR studies of crown ethers,[32,34] nonactin,[35a] and oligoethers[35b] whose structures were determined by X-ray analysis. The resonance of **4** in the solid shows similar chemical shifts, and the difference in chemical shifts in the solid and those in solution is within 2.5 ppm for other signals. Aryl−O−C torsion angles for the crown ether and **4** where the backbone is bending have very similar values, 79.9° and −76°, respectively. The signal at 118.18 ppm is assigned to C37 on the basis of value in solution and also that of benzo-9-crown-3.[32] The chemical shift of C40 would be either 68.55 or 76.12 ppm which is about 3.4−4.2 ppm different from that in solution. The ^{13}C chemical shift difference of the carbonyl carbon of **4** in the solid and in solution is 2.3 ppm. Intramolecular hydrogen bonding might affect the chemical shift.

Relationship between Structures in Solution and Ion-Transport Properties of 1. From the ^1H and ^{13}C NMR data, it is evident that the conformation of **4−6** differs from that of **2** and **3** as well as the free-acid form, **1** in chloroform. These solution structures explain the solubility, interfacial tension, and dynamic light scattering experiments well.[11] On the basis of the overall experiments, the ion-transport mechanism of **1** will be explained as follows. In a liquid membrane, **1** has high mobility as an acyclic ionophore and preorganization for the ion-transportation would not occur. Such behavior of **1** differs from that of monensin and nigericin, naturally-occurring carboxylic ionophores. It would form lipophilic complexes like the seam of a tennis ball with K and Rb ions in particular at the interface of the alkaline phase, which are not affected by a small amount of water. However, **1** cannot keep the lipophilic structures with Na^+ under a wet condition, or with Li^+ even in a dried solvent, the ions would be carried as emulsion-like aggregates. These could be the reasons why **1** possesses selectivities for K, Rb, and Cs versus Li and Na. Our results support the proposed transport mechanism and provide more information on the nature of the flexible ionophore. Such a

(32) Buchanan, G. W.; Driega, A. B.; Bensimon, C; Moghimi, A.; Kirby, R. A.; Bouman, T. D. *J. Can. Chem.* **1993**, 1983.

(33) Buchanan, G. W; Driega, A. B; Ratcliffe, C. I. *Magn. Reson. Chem.* **1993**, *31*, 1094.

(34) Belton, P. S.; Tanner, S. F.; Wright, K. M.; Payne, M. P.; Truter, M. R.; Wingfield, J. N. *J. Chem. Soc., Perkin Trans 2*, **1985**, 1307.

(35) (a) Saito, H.; Tabeta, R.; Yokoi, M. *Magn. Reson. Chem.* **1988**, *26*, 775. (b) Tabeta, R.; Saito, H. *Bull. Chem. Soc. Jpn.* **1985**, *58*, 3215.

spectral change is not seen in X-206 and nigericin, naturally occurring carboxylic ionophores having a similar backbone length.[12a,36] It seems that the contribution of the 3D structure in the crystal for **6** is less than that for **4** and **5**, which could relate to the ion-selectivity sequence. However, we need further studies to discuss such a delicate problem.

Conclusions

The solution structures of **1−6** have been studied using the ^{1}H and ^{13}C NMR data of ^3J, NOE, and chemical shifts combined with the data determined by X-ray crystallography. Although the conformation of the backbones is not strictly determined by $^3J_{H-H}$ and NOE, the use of chemical shifts additionally helps the elucidation of solution structures.

Predominance of gauche conformers around the C−C bonds of 1,2-ethylenedioxy and the observed NOE of **4−6** show a good correlation with expected results from the structures in the crystal. The observed chemical shifts agree well with those calculated on the basis of the three-dimensional structures in the crystal of **4−6**. Their chemical shifts are attributed mainly to spatial arrangements of the aromatic rings. On the basis of the ^{13}C NMR spectra in solution, the backbone bending of **4−6** observed in the crystal is also confirmed with $^3J_{H-C}$ and chemical shifts. The solid-state NMR of **4** shows spectral patterns similar to those in solution.

These ^{1}H and ^{13}C NMR data show that the contribution of the 3D structure in the crystal for **4−6** is dominant, whereas a large number of conformers are rapidly interconverted on the NMR time scale for the free-acid ionophore and the Li and Na salts. These results are in accordance with the solubility of **1−6** in chloroform[10d] and would explain why **1** transports K^+, Rb^+, and Cs^+ more than Li^+ and Na^+.

Experimental Section

Materials. The following reagents were used as received: $CHCl_3$, MeOH, LiOH, NaOH, KOH, and KBr (Wako Pure Chemical Industries, Ltd.), RbOH and CsOH (Kanto Chemical Co. Inc.), and $CDCl_3$ (99.5%) and tetramethylsilane (TMS) (E. Merck).

The synthesis of ionophore **1** has been previously described.[10d−f,11] The alkali metal salts were prepared by neutralization of **1** dissolved in methanol with the corresponding alkali metal hydroxides followed by drying in vacuo.[11] The formation of alkali metal salts of **1** was identified by lower-shifts of $\nu_{C=O}$ in IR spectra.

NMR samples except those for the LRJR measurement were prepared

at concentrations of 10−20 mM in $CDCl_3$ solution. For the LRJR measurement, the sample was prepared at a concentration of 136 mM. In measuring the NOE, samples were vacuum-degassed using the freeze−pump−thaw technique and the sample tubes were sealed before use.

Instrumentation. Infrared spectra (KBr disks) were recorded on a JEOL JIR-AQS20M FT-IR spectrometer at 25 °C.

[1]H (500.00 MHz), [13]C (125.65 MHz—complete ^{1}H noise decoupling), and 2D-NMR spectra (COSY, NOESY, and LRJR) were recorded in 5 mm ϕ tubes on a JEOL GSX-500 FT-NMR spectrometer. HMQC and HMBC ($^3J_{C-H}$ = 5.5 Hz) were recorded in 5 mm ϕ tubes on a JEOL EX-400 FT-NMR spectrometer. NOE intensities were measured in 5 mm ϕ tubes on JEOL GX-400 (for **4**), a GSX-500 (for **5**), and a EX-400 (for **6**) FT-NMR spectrometers as subtraction of nonirradiated spectra from irradiated ones. Chemical shifts of ^{1}H NMR were measured from TMS as the internal standard in $CDCl_3$ solution within ±0.46 Hz experimental error and those of ^{13}C NMR from $CDCl_3$ (77.1 ppm) within ±0.95 Hz experimental error. Only the LRJR measurements were carried out at 40 °C. The other measurements were done at 25 °C.

The high-resolution solid-state ^{13}C NMR spectra (67.80 MHz) were recorded at 25 °C on a JEOL GSX-270 FT-NMR spectrometer, utilizing an accessory for cross polarization magic-angle spinning (CPMAS). Each sample (ca. 300 mg) was contained in a rotor and spun at up to 6 kHz by compressed air. The duration of the 90° pulse, the contact time, and the recycling time were 4.2 μs, 2 ms, and 5.038 s, respectively. Spinning side bands were removed by the pulse sequence for the total suppression of spinning side bands (TOSS).[37] The chemical shifts were referred to external adamantan and converted to the TMS scale by a factor of 29.5 ppm.

Supporting Information Available: Tables listing the chemical shifts of ^{1}H and ^{13}C NMR spectra of **1** and its alkali metal salts (4 pages). This material is contained in libraries on microfiche, immediately follows this article in the microfilm version of the journal, can be ordered from the ACS, and can be downloaded from the Internet; see any current masthead page for ordering information and Internet access instructions.

JA950683W

(36) (a) Van Roey, P.; Duax, W. L.; Strong, P. D.; Smith, G. D. *Isr. J. Chem.* **1984**, *24*, 283. (b) Anteunis, M. J. O. *Bull. Soc. Chim. Belg.* **1977**, *86/n*, 931.

(37) Dixon, W. T. *J. Chem. Phys.* **1982**, *77*, 1800.